RESEARCH ARTICLE

Variability of SO_2, CO, and light hydrocarbons over a megacity in Eastern India: effects of emissions and transport

**Chinmay Mallik · Dipanjan Ghosh · Debreka Ghosh ·
Ujjaini Sarkar · Shyam Lal · S. Venkataramani**

Abstract The Indo-Gangetic plain (IGP) has received extensive attention of the global scientific community due to higher levels of trace gases and aerosols over this region. Satellite retrievals and model simulations show that, in particular, the eastern part IGP is highly polluted. Despite this attention, in situ measurements of trace gases are very limited over this region. This paper presents measurements of SO_2, CO, CH_4, and C_2–C_5 NMHCs during March 2012–February 2013 over Kolkata, a megacity in the eastern IGP, with a focus on processes impacting their levels. The mean SO_2 and C_2H_6 concentrations during winter and post-monsoon periods were eight and three times higher compared to pre-monsoon and monsoon. Early morning enhancements in SO_2 and several NMHCs during winter connote boundary layer effects. Daytime elevations in SO_2 during pre-monsoon and monsoon suggest impacts of photo-oxidation. Inter-species correlations and trajectory analysis evince transport of SO_2 from regional combustion sources (e.g., coal burning in power plants, industries) along the east of the Indo-Gangetic plain impacting SO_2 levels at the site. However, C_2H_2 to CO ratio over Kolkata, which are comparable to other urban regions in India, show impacts of local biofuel combustions. Further, high levels of C_3H_8 and C_4H_{10} evince the dominance of LPG/petrochemicals over the study location. The suite of trace gases measured during this study helps to decipher between impacts of local emissions and influence of transport on their levels.

Keywords Sulfur dioxide · Carbon monoxide · Hydrocarbons · Emission characteristics · Transport effects · Regional and local sources

Introduction

The atmospheric environment over a region is an open system with respect to trace gas concentrations, being affected by both local and regional contributions. These contributions are a result of the coupling between emission and transport processes, which vary with region of the atmosphere and season of the year. Further, trace gas levels over a location are also affected by chemistry, photochemistry, dynamics, and meteorology. The characterization of local variability becomes very important over major urban regions viz. megacities which are major sources (and sometime sinks) for a plethora of species affecting chemistry and budget at regional to global scales. The characterization is better elucidated if measurements involve multiple chemical species, which can serve as proxies for different source and sink terms. Some of these gases, e.g., ozone (O_3), nitrogen oxides (NO_x), carbon monoxide (CO), methane (CH_4), non-methane hydrocarbons (NMHCs), sulfur gases including sulfur dioxide (SO_2), etc. play important roles towards various atmospheric processes that affect the overall state of our health and ecosystem.

Measurements of SO_2 are highly desirable over urban regions as it colligates important aspects of air pollution, atmospheric chemistry, and climate. It is a primary criteria pollutant with potentially adverse health effects and concomitant deleterious impacts on the flora and fauna. It is a precursor of sulfate aerosols which exert a direct radiative forcing (RF) of -0.40 ± 0.20 W m^{-2} (Forster et al. 2007). One half to

C. Mallik · S. Lal (✉) · S. Venkataramani
Space and Atmospheric Sciences Division, Physical Research Laboratory, Ahmedabad, India
e-mail: shyam@prl.res.in

D. Ghosh · D. Ghosh · U. Sarkar
Department of Chemical Engineering, Jadavpur University, Kolkata, India

two thirds of this RF is attributable to anthropogenic sulfur (mainly SO$_2$). Despite global reductions in SO$_2$ emissions, a 70 % growth is estimated over India during 1996–2010 (Lu et al. 2011). Ninety-one percent of these emissions are attributed to power-plants and industries (emitting 5,236 and 2,784 Gg SO$_2$, respectively, in 2010). Various emission sources of SO$_2$ are presented in Table 1. Garg et al. (2001) have estimated that power generation alone accounts for 46 % of total SO$_2$ emissions in India. Annual electricity consumption in India is 600 million MWh (http://www.indexmundi.com/map/) with 7,000 tonnes SO$_2$ emitted for every megawatt hour of electricity produced. Most of this electricity (about 60 %) comes from coal based thermal power plants. Annual coal (0.2–0.7 % S) consumption in India is around 340 Mt (http://www.eai.in/ref/fe/coa/coa.html). SO$_2$ emissions from the oil sector vary between 0.5 and 8 % (Garg et al. 2001), the highest being for fuel oil. India consumed about 1,165 million barrels of crude oil (includes heating oil, gasoline, diesel, etc.) during 2012. On average, petroleum refineries in India emit about 48 tonnes of SO$_2$ for every 1,000 barrels of production.

The importance of CO and NMHCs in controlling tropospheric O$_3$ is very well documented. These gases also wield substantial influence on air quality and global climate. Being important consumers of hydroxyl radicals, they can enhance the lifetime of atmospheric greenhouse gases. Documentation of their levels over major emission regions like mega-cities is very important due to potentially large fluxes. The major sources of CO and NMHCs are presented in Table 1. It is to

be noted that systematic representative measurements of SO$_2$, CO, and NMHCs are still limited to very few locations in India (Tables 2 and 3), and hence knowledge about their abundance and variability could have cornerstone implications to the understanding and modeling of tropical, atmospheric chemistry. In the present paper, we report a year-long observation of SO$_2$, CO, CH$_4$, and NMHCs (C$_2$–C$_5$) over the megacity "Kolkata", an urban region in Eastern India (Fig. 1). Being located in tropical South Asia, Kolkata can significantly influence the regional chemistry. Based on multi pollutant index (MPI) studies, the air quality of Kolkata is worse than several other megacities of the world (Gurjar et al. 2008). High levels of pollutants during winter over Kolkata are also clearly observed from surface measurements (Mallik and Lal 2013) as well as satellite measurements of CO. Electronic supplementary material (ESM) Fig. 1 shows that during April, high levels of CO are observed over Bangladesh (east of Kolkata) whereas during winter, high levels of CO occurs over Kolkata. Further, satellite based CO measurements clearly show higher levels over the eastern part of the Indo-Gangetic plains (IGP). The outflow of IGP pollution into the Bay of Bengal (BoB) occurs over this region as the winds turn towards south instead of going further east (Mallik et al. 2013). Thus, it is apt to describe Kolkata as the gateway for air pollutants from the IGP to the BoB during winter and post-monsoon and vice versa during monsoon and pre-monsoon. From the perspective of emission inventories, these measurements can characterize a major emission source region in Eastern India.

Table 1 Sources of SO$_2$, CO, CH$_4$, and NMHCs

Species	OH rate constant at 298 K 10^{-12} (cm^3 molec^{-1} s^{-1})	Sources		Reference
		Major	Other	
SO$_2$	1.1	Coal in power plants, industries (steel, cement)	Petroleum refineries, chemical and metal industries, transport sector	Garg et al. (2001) Streets et al. (2003)
CO	0.15–0.21	Biofuel and biomass burning Incomplete combustion of fossil fuel (gasoline vehicles)	Oxidation of CH$_4$ and other hydrocarbons	Streets et al. (2003) Duncan et al. (2007)
CH$_4$	0.0063	Agriculture, livestock, wetland	Landfill, coal mines, natural gas, biomass/biofuel	Streets et al. (2003) Wang et al. (2004a)
C$_2$H$_6$	0.26	Biofuel/biomass, natural gas	Fossil fuel (coal), oceans	Rudolph (1995)
C$_2$H$_4$	8.52	Biomass/biofuel	Fossil fuel (with ethanol), petrochemical (plastic, etc.)	Sawada and Totsuka (1986) Horowitz et al. (2003)
C$_2$H$_2$	0.82	Transport sector (biofuel/fossil fuel)	Biomass	Xiao et al. (2007)
C$_3$H$_8$	1.15	Fossil fuel (LPG)	Petrochemical industry, natural gas	Duncan et al. (2007) Blake and Rowland (1995)
C$_3$H$_6$	26.30	Fossil fuel/biofuel	Biomass petrochemical (plastic, etc.)	Duncan et al. (2007)
C$_4$H$_{10}$	2.44	Fossil fuel (LPG), petrochemical industry	Biomass/biofuel solvent usage	Horowitz et al. (2003) Guo et al. (2007)
C$_5$H$_{12}$	3.90	Vehicles (gasoline evaporation)		Guo et al. (2007) Xie and Berkowitz (2006)

Table 2 Average concentrations of SO_2 (parts per billion by volume) over different regions in India and the world. Summer (s; premonsoon) and winter (w). Most of the datasets are based on continuous monitoring (UV Fluorescence) method. The data for Mumbai is based on samples collected once a month and analyzed using West and Gaeke method. The data for Europe is based on chemical ionization mass spectrometry

Station	Kolkata	Ahmedabad	Mumbai	Delhi	(Yuen Long) Hong Kong	Lin'an (China)	Seoul (Korea)	Beirut (Lebanon)	East Europe
Period	1 Mar 2012–28 Feb 2013	14–26 May 2010	Jan 1997–Dec 2000	Jan–Dec 2008	Sep 2002–Aug 2003	2007–2008	1998–2003	Sep 2004–Feb 2005	1 Jun–6 Jul 2000
Mean	0.8 (s) 6.4 (w)	0.95 (s)	9.6	1.48 (s) 2.55 (w)	6.2	12.3	7.9	4.9 (s) 9.4 (w)	0.52
Sigma	0.4 (s) 4.6 (w)	0.88	2.0				2.6		0.47
Maximum	3.6 (s) 40.4 (w)	17	52.3				15.0	22.5	8.5
n	2,083 (s) 2,146 (w)	302	500				72	4,320	
	This study	Mallik et al. (2012)	Gupta et al. (2003)	Datta et al. (2011)	Guo et al. (2007)	Meng et al. (2010)	Nguyen and kim (2006)	Saliba et al. (2006)	Hanke et al. (2003)

Methodology

The study location

The study was conducted in Kolkata (formerly Calcutta; 22.55°N, 88.50°E; 6 m amsl), a megacity in Eastern India, spread over an area of 1900 km² with population of about 15.7 millions. Kolkata is the capital city of the West Bengal state of India (Fig. 1). The port of Kolkata has two major dock agglomerations at Kolkata and Haldia. Haldia is a major port city, about 120 km south-west of Kolkata with a major refinery. Durgapur and Asansol are two other major industrial townships about 170 and 210 km to the north-west of Kolkata. Huge power plants lie within a few hundred kilometers in the north-west of Kolkata. The study site is located in the lush green campus of Jadavpur University at Salt Lake, a planned township in East Kolkata, with mostly office and residential buildings. The city itself has a few small-scale industries mostly located in the south-west of the study location. Dhapa, located south of the study location, is a major landfill site for dumping solid wastes of Kolkata. A major international airport is located within 10 km north of the study location. Public transport is more favored in Kolkata than private vehicles. Excluding two-wheelers (0.18 million) and cars (0.19 million), the city has about 0.45 million registered motor vehicles constituted by trucks (20 %), buses (6 %), taxi (45 %), and auto-rickshaws (28 %) (http://morth.nic.in/index2.asp?slid= 291&sublinkid=137&lang=1). Most of these vehicles run on diesel, auto-rickshaws run on compressed natural gas (CNG) while two-wheelers and cars run on petrol (gasoline).

Experimental details

Continuous in situ measurements of surface SO_2 were made over Kolkata during March 2012–February 2013, using an online gas analyzer from Thermo Scientific (43i-TLE). It is based on UV fluorescence (USEPA Equivalent Method EQSA-0486-060; http://www.epa.gov/ttn/amtic/criteria.html) and achieves a detection limit of 50 pptv for a 300-s averaging time. Ambient air is drawn through 4-m-long PTFE tubing (5-mm ID) into the analyzer through a 5-μm PTFE filter (to remove dust). The air then passes through a hydrocarbon kicker which removes hydrocarbons that fluoresce in the same region as SO_2 (Mohn and Emmenegger 2001). The SO_2 molecules are then excited by UV radiation (214 nm). The resulting fluorescence is measured by a PMT. Periodic zero calibration of the analyzer is carried out using zero air cylinders from British Oxygen Corporation, India, and a series of purafil/molecular sieve scrubbers. Span calibrations are done by diluting a gas mixture from Intergas (International Gases & Chemicals), UK (concentration: 471 ppbv in N_2, traceable to National Physical Laboratory, UK) and a multi-gas calibrator (MCG146i; Thermo Scientific, USA).

Table 3 CO, CH$_4$, and NMHCs (parts per billion by volume) over different regions in India and the world. The Ahmedabad data is based on direct online GC measurements for periods stretching 72 h (1-h interval) for each month

Station Year No. of samples	Kolkata Mar 2012–Feb 2013 71	Ahmedabad Jan–Dec 2002 Online	Mumbai Mar 1993–May 1994 260	Hydera bad Jan–Dec 2010 ~300	Mt. Abu Jan–Dec 2002	Karachi 10 Dec 1998–11 Jan 1999 78	NE-China 20 Jun–13 Jul 2007 8	Hong Kong Sep 2002–Aug 2003 62	Mexico City Mar 2006 200	London 1 Jan 1998–31 Dec 2008
CO	677±194	385±200	–	–	131±36	1,600±1,300	645±449	511	1,862±1,352	530
CH$_4$	2,259±210	1,880±400	–	–	1,630±40	6,300±4,700		2,024	2,880±1,140	–
C$_2$H$_6$	3.9±3.4	3.7±3.7	1.3	28.3	1.2±0.6	93±84	3.0±1.6	2.1	13.9±11.7	7.1
C$_2$H$_4$	4.5±2.9	2.9±2.6	2.3	3.1	0.3±0.2	19±17	2.8±2.3	2.7	13.9±11.4	2.4
C$_2$H$_2$	3.7±2.5	2.0±1.9	1.1	2.6	0.4±0.4	18±16.2	4.0±5.0	2.9	16.3±13.1	1.3
C$_3$H$_8$	8.4±5.6	4.4±2.9	5.6	3.5	0.5±0.2	41±35	1.9±1.2	2.5	78.3±64.3	2.7
C$_3$H$_6$	1.8±1.7	1.0±0.9	0.2	–	0.2±0.1	5.5±5.3	1.1±1.6	0.6	4.0±3.6	0.7
i-C$_4$H$_{10}$	4.0±3.6	1.9±1.5	5.3	–	0.2±0.2	11±9	0.9±0.7	1.5	11.7±9.8	1.2
n-C$_4$H$_{10}$	6.3±5.0	2.8±2.4	16.4	2.4	0.3±0.3	19.8±16	1.0±0.6	2.6	33.1±24.6	2.0
i-C$_5$H$_{12}$	3.2±2.2	1.9±2.4	–	7.7	–	12.1±11.6	1.2±1.1	1.1	9.2±7.5	1.6
	This study	Sahi and Lal (2006a)	Rao et al. (1997)	Swamy et al. (2012)	Naja et al. (2003) Sahu and Lal (2006b)	Barletta et al. (2002)	Xue et al. (2011)	Guo et al. (2007)	Apel et al. (2010)	Schneidemesser et al. (2010)
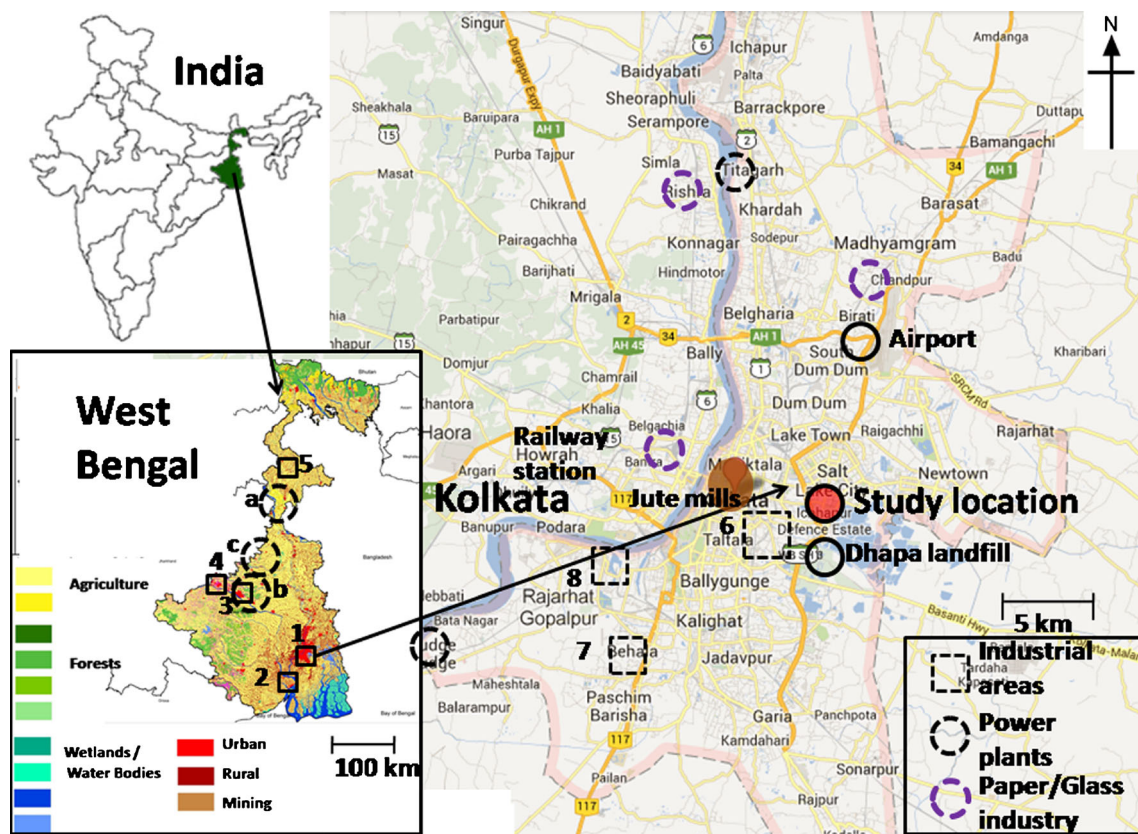
Fig. 1 The study location in (*1*) Kolkata (*city map on the right*). Major power plants (*a*) Farakka (2,100 MW), (*b*) Menjia (2,340 MW), (*c*) Bakreshwar (1,050 MW). Industrial areas: (*2*) Haldia (petrochemicals), (*3*) Durgapur (steel industry), (*4*) Asansol (steel, locomotives), (*5*) Raniganj (coal fields). Industrial areas in Kolkata: (*6*) Kasba, Tangra, Beliaghata (leather, polymer); (*7*) Behala, Taratala, Majerhat (engineering, pharmaceuticals, food); (*8*) Garden Reach (ship builders). Budge-Budge thermal power station (750 MW) lies 40 km south-west of study location. Kolaghat thermal power station (1,260 MW) is 40 km to west of Budge-Budge (not shown in map)

In addition to the online SO_2 measurements, 71 air samples were collected during February 2012–February 2013, for offline GC analysis. The air samples were collected from 4 m above ground level using a Teflon tube at 3-h intervals between 0730 to 1930 IST into pre-evacuated (to 10^{-5} mbar) 900-ml borosilicate glass sampling bottles using an oil-free air compressor (MB-158-E, Metal Bellow, USA). The Indian Standard Time (IST) is 5 h and 30 min ahead of Greenwich Mean Time (GMT). Each bottle was flushed several times with the ambient air before finally filling the sample to a pressure of around 2.5 bar leading to sample sizes of about 2.25 L (STP) each. These samples were analyzed in the laboratory at PRL, Ahmedabad for CH_4, CO, and light NMHCs (C_2–C_5), using gas chromatographic methods given in Sahu and Lal (2006a), within a month of sampling at Kolkata. The stability tests regarding storage of these hydrocarbons showed variations of the order of 4–5 % w.r.t. the mean for a 2-month period (ESM Fig. 2). The response of the FID detector was found to be linear over the range 100 pptv to 60 ppbv for ethane (C_2H_6), ethene (C_2H_4), propane (C_3H_8), propene (C_3H_6), acetylene (C_2H_2), *n*-butane (*n*-C_4H_{10}), *i*-butane (*i*-C_4H_{10}), and *i*-pentane (*i*-C_5H_{10}). The reproducibility in

NMHCs analyses ranged between 3 and 10 % depending upon the compounds, in general lower molecular weight hydrocarbons showed better reproducibility.

Auxiliary data sources

Hourly means of temperature, relative humidity, wind speed, and direction during March 2012–February 2013 from the nearby Kolkata Airport were used for the analysis. In addition to this, daily data for surface wind components (zonal, meridional; in meter per second), omega (in Pascal per second), and lifted index (degree kelvin) over 22.5°N, 87.5°E were obtained from 2.5°×2.5°-resolution NCEP reanalysis (http://www.esrl.noaa.gov/psd/data/gridded/data.ncep.reanalysis.surface.html). Trajectory data and boundary layer heights were obtained from NOAA archives using HYSPLIT (http://ready.arl.noaa.gov/HYSPLIT.php). Further, SO_2 mass mixing ratios (in kilogram per kilogram) and columnar dust AOD at 550 nm were obtained from European MAAC model reanalysis (22.5°N, 88.5°E; http://data-portal.ecmwf.int/data/d/macc_reanalysis/) for comparison. CO mixing ratios (1°×1° monthly gridded, level 3) are obtained from "Measurements

Of Pollution In The Troposphere" (MOPITT) for the year 2012 (ftp://l4ftl01.larc.nasa.gov/MOPITT/MOP03M.004.).

Results and discussion

Wind pattern over Kolkata during the study period

The prevailing wind patterns over Kolkata during the study period are shown in Fig. 2. Based on their spatial coverage, the air masses may be divided into three major types. During premonsoon (March, April, May), Kolkata is influenced by low-level southerly air masses from the Bay of Bengal and coastal India. These air masses spend 75 % time below 500 m and 15 % time between 500 and 1,000 m. During monsoon (June, July, August, and early September), the wind regime shifts to south-westerly and brings air parcels from southern peninsular India. These air parcels spend about 64 % time below 500 m, 18 % time between 500 and 1,000 m and 15 % time between 1,000 and 2,000 m. A complete reversal of winds takes place during late September (ESM Fig. 3). During the post-monsoon (late September, October, November), wind is mostly north-westerly over the study location. During winter (December, January, February), the prevailing wind-pattern is same as during post-monsoon, bringing in air masses from the IGP. Reversal of winds again takes place in March. During post-monsoon, air masses reside about 37 % time below 500 m, 21 % time between 500 and 1,000 m and 35 % time between 1,000 and 3,000 m. The residence times during winter are 37 % below 500 m, 31 % between 500 and 1,000 m and 28 % between 1,000 and 3,000 m. During pre-monsoon, the trajectories reside 89 % time over oceans whereas during monsoon, this value reduces to 43 %.

Seasonal variation in surface SO₂

Hourly average SO_2 concentrations are calculated from 5-min averages recorded by the instrument. A comparison of SO_2 values obtained over Kolkata with other locations is presented in Table 2. The median concentrations of SO_2 for Kolkata are 0.8 for premonsoon and 5.2 during winter. Assuming local emissions do not change much throughout the year, the several fold increase in winter concentrations seem to be a result of atmospheric dynamics (meteorology and regional transport). The median concentration of SO_2 over Kolkata during premonsoon is slightly higher than median concentration observed over Ahmedabad (0.6; Mallik et al. 2012). The median SO_2 concentration observed over Mumbai over a 4-year sampling period was, however, 7.5 ppbv. The mean winter concentrations of SO_2 over Kolkata are comparable to concentrations observed over Seoul and Hong Kong (Table 2).

The variation in observed hourly average SO_2 concentrations as a function of wind direction is shown in Fig. 3. It is clearly observed that the hourly SO_2 concentrations during post-monsoon (mean=3.5 ppbv) and winter (mean=6.4 ppbv) are far higher than those during pre-monsoon (mean=0.83 ppbv) and monsoon (mean=0.72 ppbv). From the figure, there seems to be a dominant effect of prevailing wind regimes, resulting in

Fig. 2 Seasonal patterns of prevailing winds over Kolkata. One hundred twenty-hour backward trajectory data from HYSPLIT are grouped into three major regimes representing pre-monsoon (March–May), monsoon (June–August) and post-monsoon+winter (late September–February). The altitude of these trajectory groups is shown by the *color bar*. The *colored circles* represent power plants (which are large point sources for SO₂). *Size and color of the circles* are scaled according to the capacity of the power plants; e.g., the Mudra Thermal power station in western Gujarat, fifth largest single location coal-based thermal power, has an installed capacity of 4,620 MW
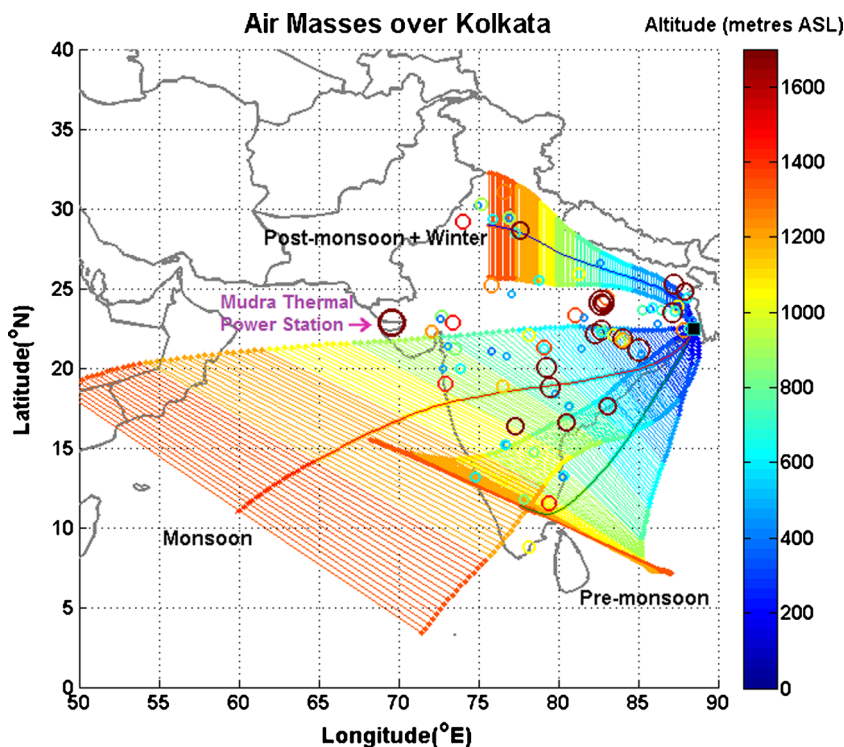
different catchment areas for SO_2 during the different periods. During post-monsoon and winter, sources are mainly in north and north-west (also Fig. 4a). Decent correlations between daily means of SO_2 and zonal wind (R^2=0.23 and 0.31 during winter and post-monsoon; n=90 for each season) and a skewed distribution of SO_2 with wind direction indicate a regional influence. Further, a sudden change in SO_2 levels is observed towards the end of September, along with a concurrent change in wind regime (ESM Fig. 3). This change is also reciprocated by the MAAC simulations (ESM Fig. 4). There seems to be an association between SO_2 and lifted index (LI; a measure of atmospheric stability) during post-monsoon (slope=0.43, R^2=0.67, n=90). During this period, SO_2 values start to increase as the LI values change from negative to positive, i.e., atmosphere becomes more stable.

The regional sources potentially contributing to higher SO_2 concentrations during January and July are shown in

Fig. 4a, b). These maps are based on potential source contribution function (PSCF) analysis (Wang et al. 2009). Figure 4a shows that SO_2 concentrations greater than 75 percentile of January values are related to air masses passing over steel industries in Bokaro and Durgapur, coal mining regions of Jharia and Raniganj, apart from numerous other industrial townships and polluted areas in West Bengal, Jharkhand, Bihar, and Uttar Pradesh. These air masses also intersect with numerous power plants including Menjia (2,340 MW), Farakka (2,100 MW), and Bakreshwar (1,050 MW). Previous modeling studies have also shown these regions as hotspots for SO_2 emissions (Adhikary et al. 2007). Coal combustion in power plants and steel industries are major contributors to regional SO_2. Figure 4b shows that SO_2 concentrations greater than 75 percentile of July values are related to air masses coming from the industrial townships of Haldia and Paradeep.
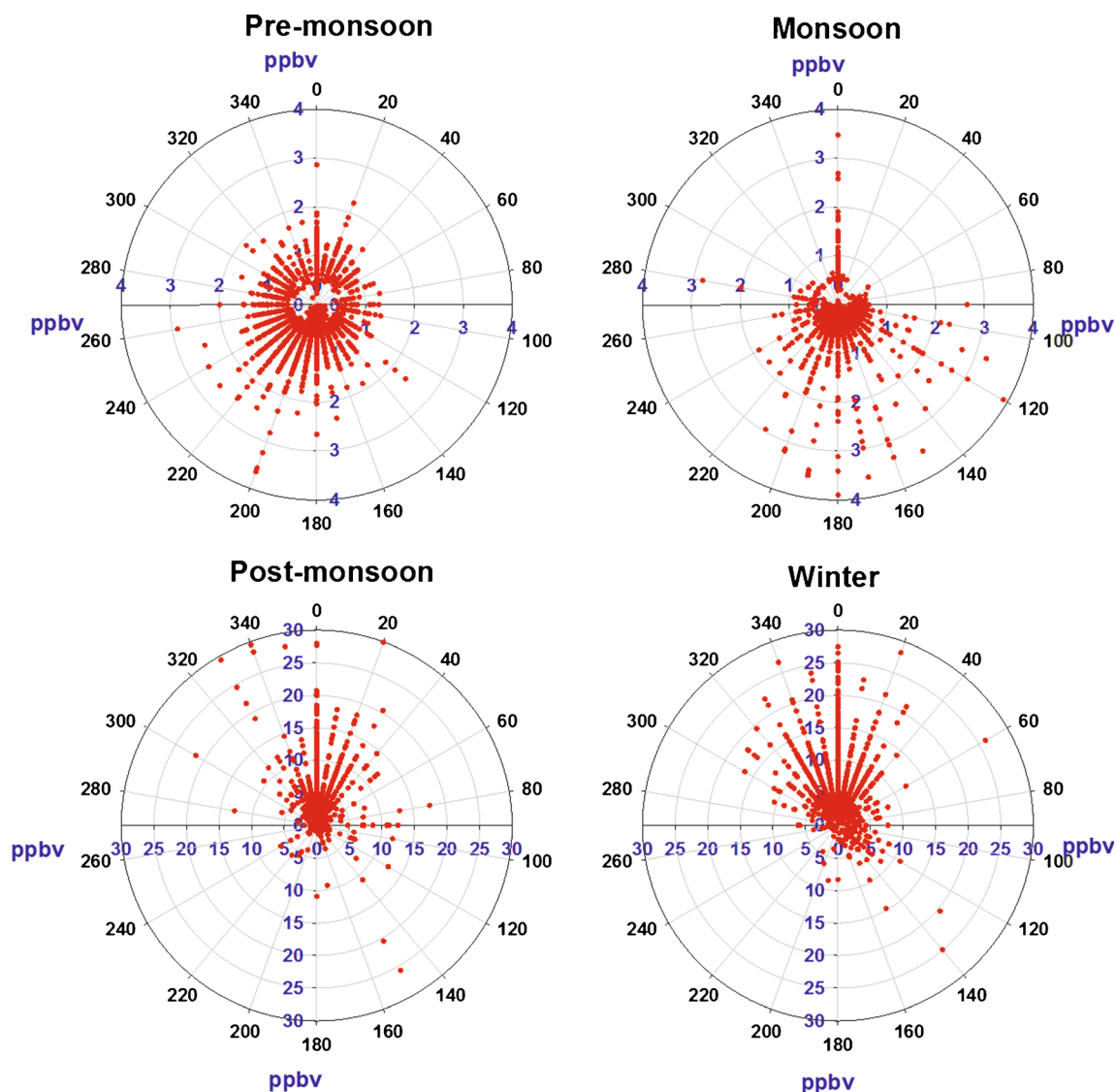
Fig. 3 Variation of hourly SO_2 (parts per billion by volume) with wind direction during different seasons over Kolkata during the study period

Fig. 4 Probable source regions contributing to elevated SO$_2$ concentrations over the study location during **a** January and **b** July. The maps are derived from Potential source contribution function analysis using TrajStat software (Wang et al., 2009). Runtime, 120 h, cell size=2°×2°. Pollution criteria, 75 percentile of monthly variation of SO$_2$. The *red grids* represent a probability of 0.7–1, followed by pink (0.42–0.7) and orange (0.17–0.42)
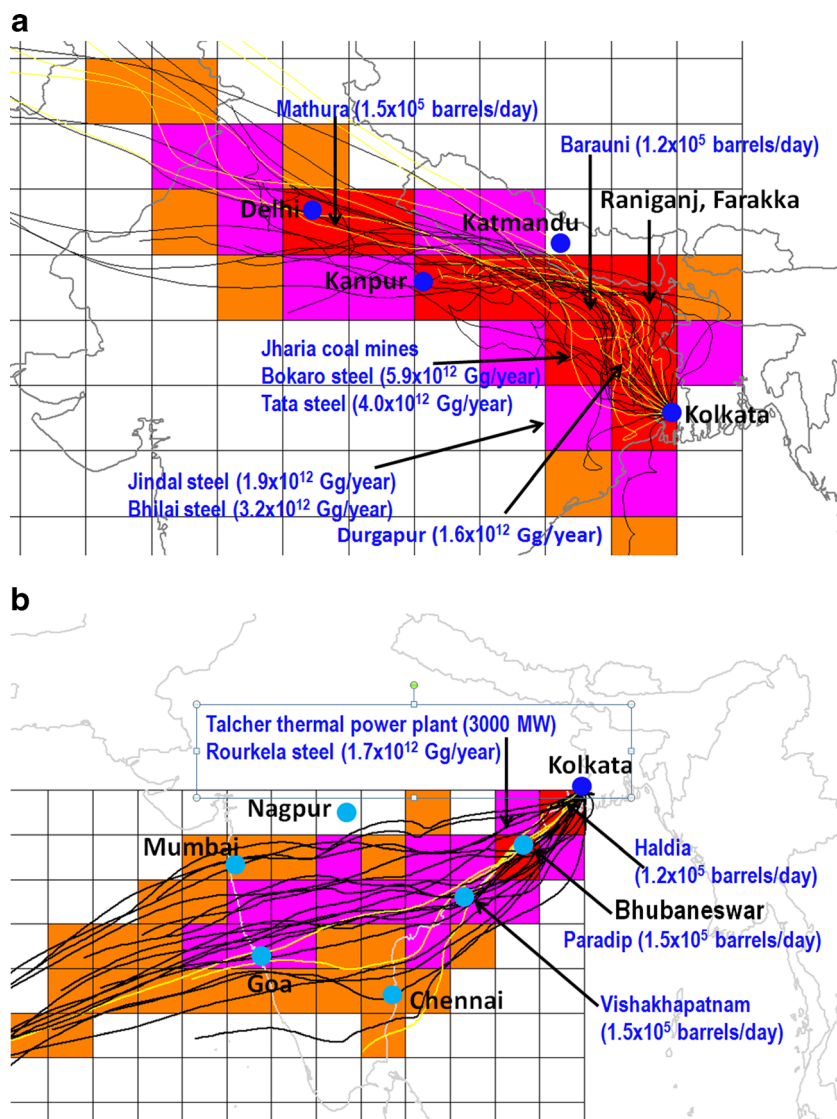

The average SO$_2$ concentration during March–August is about 0.8 ppbv, which is about 16 % of the average concentration during September–February (4.9 ppbv). This is because the air masses during winter pass over more polluted regions of the IGP. Although numerous power plants lie in the catchment area for SO$_2$ during March–August (Fig. 2), dilution effect is larger during this period. Meng et al. (2010) attribute lower SO$_2$ concentrations during summer at several Chinese sites to vertical mixing and removal mechanisms (precipitation, photochemical). Dilution effects can be measured from ventilation coefficient (VC), obtained by multiplying wind speed with mixed layer depth (MLD). In source regions such as megacities, VC represents the rate by which pollutants will be blown out of the mixed layer over a particular location. Chin and Jacob (1996) have estimated that ventilation accounts for 90 % of SO$_2$ export from USA to the free troposphere in summer while this reduces to 30 % in winter. MLD values over the study location are generally

below 500 m during winter and post-monsoon but extend to 2,000 m and above during pre-monsoon and monsoon. Further, wind speeds are higher over Kolkata during monsoon and pre-monsoon (mean=3.4 m/s) accentuating the VC values during these periods. Thus higher VC during pre-monsoon will cause dilution of local emissions while lower VC during winter and post-monsoon results in stronger trapping of transported air parcels from other source regions as well as local emissions. Figure 5 confirms that higher SO$_2$ concentrations generally occur at lower VC. However, the correlations of SO$_2$ with VC or MLD are not strong enough to quantify their effects.

Apart from the effect of source contributions, removal mechanisms play a vital role in governing ambient SO$_2$ levels. The major sinks are oxidation, dry-deposition, and wet-deposition, with global average contributions of 53, 36, and 8 %, respectively (Faloona 2009). The columnar dust AOD at 550 nm over Kolkata during summer is 0.36, which is about
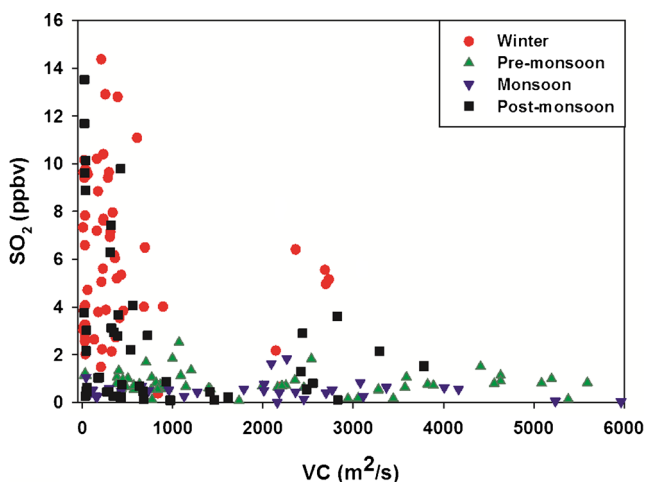
Fig. 5 Variation of SO_2 with ventilation coefficient

45 % higher than winter average (0.25) and could result in higher heterogeneous losses of SO_2. Adhikary et al. (2007) have discussed the importance of heterogeneous pathways in conversion of SO_2 to sulfate over the Indian region, especially during the dry season. Guttikunda et al. (2001) have also estimated high sulfur deposition over the Indian region during summer. High SO_2 dry deposition velocities were calculated over China during summer (0.45 cm/s; Wang et al. 2003). The efficacy in wet removal processes in determining SO_2 concentrations over heavy rainfall areas like Kolkata could be significant during monsoon (Matsuda et al. 2006). Rai et al. (2010) have calculated a deposition rate of 185 $\mu g\ m^{-2}\ s^{-1}$ for SO_2 removal at a rainfall rate of 168 mm/h. However, more detailed analysis is needed to quantify these effects.

Diurnal variation in surface SO_2

The monthly, diurnal patterns for SO_2 are constructed from averaged hourly data for all days of the month. Virtually, no diurnal variation in SO_2 is observed during March and August. During premonsoon and monsoon, under the southerly wind regime (180°, Fig. 3), elevated daytime values in SO_2 are observed (Fig. 6). Daytime enhancement in SO_2 envisages effects of photochemistry. Daytime enhancements in SO_2, observed at Hawaii (De Bruyn et al. 2006), were attributed to oxidation of reduced sulfur compounds (RSCs; mainly DMS). It was shown in Fig. 1 that vast landfill regions exist to the exact south of the study location within 5-km distance. Figure 3 shows elevated SO_2 concentrations when wind is coming from south during premonsoon and monsoon. Thus, oxidation of RSCs (which have major sources in landfill sites) may be surmised. There could also be other anthropogenic sources of SO_2 but their emissions will occur both during day and night. Nevertheless, the hypothesis regarding photo-oxidation of RSCs leading to daytime enhancements in SO_2 needs to be excogitated with quantitative estimations over several years.

Early morning enhancements are observed during September along with hint of late afternoon peaks. These early morning and afternoon to evening enhancements become very prominent in post-monsoon months of October and November (Fig. 6). Daytime dip in SO_2 concentrations occur during winter and post-monsoon. These daytime dips are conspicuous during October and November and could be the result of boundary layer dilution. Similar features were also observed at Lin'an, China (Wang et al. 2004b). High SO_2 concentrations during winter mornings (~8 IST) could be a result of colligated impacts of local emissions and boundary layer dynamics. During February, a gradual increase in SO_2 concentrations from midnight to early morning seems to be a clear effect of decreasing MLD. Absence of evening peaks during winter asserts that vehicular traffic does not significantly impact SO_2 concentrations over this region. A weekday to weekend ratio analysis shows that the median values are close to 1 during the study period. However, these values are much lower than 1 during winter and post-monsoon, suggesting more pre-dominant impacts of regional sources (power plants and industries which prevent the increase of weekday values) rather than local emissions (vehicular etc. which tend to increase weekday values).

Variations in CO, CH_4, and NMHCs

Figure 7 shows the diurnal variation of CO and hydrocarbons over Kolkata based on seasonal means for 0730, 1030, 1330, 1630, and 1930 IST observations. Similar to MOPITT observations (ESM Fig. 1), CO values in surface measurements are always elevated during winter compared to pre-monsoon (Fig. 7). Further, the daytime patterns in hydrocarbons during winter reveal high values during morning and evening. The morning values seem to be more related to atmospheric stability conditions rather than traffic activity (which should have peaked between 0900 and 1100 IST). Mixed layer height is lower during winter mornings compared to summer mornings, resulting in lower dilution of accumulated pollutants during night, leading to higher concentrations of hydrocarbons at 0730 IST. Further, it is clearly observed from Fig. 7 that unlike other gases, daytime concentrations (excluding morning and evening) of C_2H_4 and C_3H_6 are comparable for premonsoon and winter. However, early morning values (0730 IST) for these gases are far higher in winter than premonsoon, pointing to non-vehicular influences. The peak traffic hours in the morning (0900–1100 IST) are marked by elevated i-C_5H_{10} values, pointing to gasoline evaporation.

The average concentrations of CO, CH_4, and NMHCs over Kolkata during the study period are presented in Table 3. A comparison has been made with other available measurements in India and some other urban regions of the world. It is observed that CO and C_2H_6 levels over Kolkata are

Fig. 6 Diurnal variations of SO_2 during different seasons. The *boxes* represent the 25 and 75 percentiles
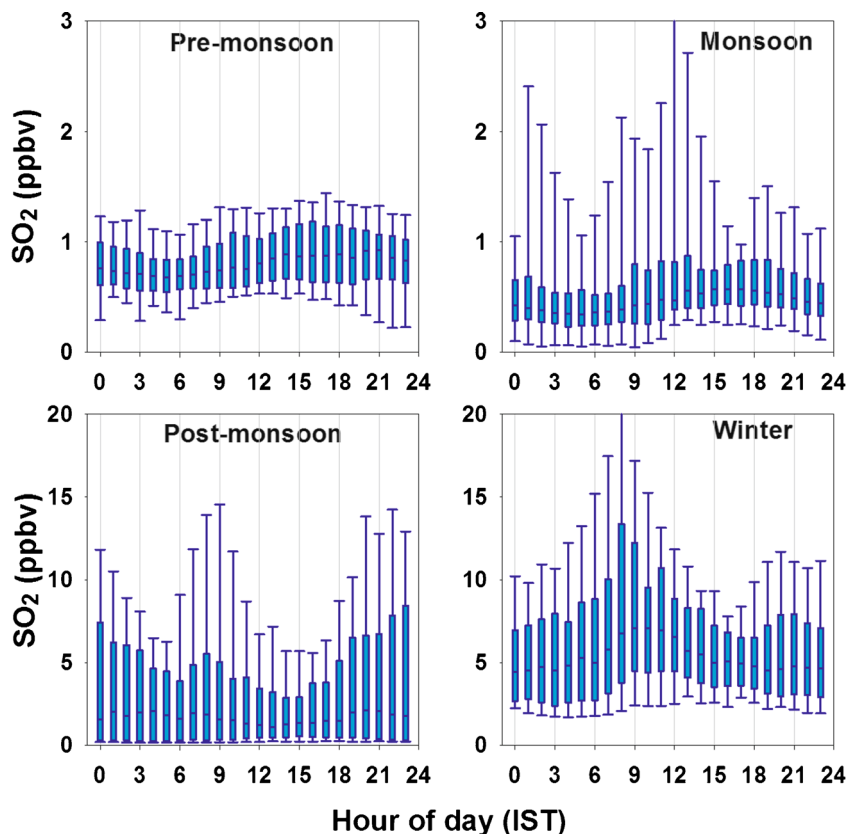
comparable to several Chinese sites while C_3H_8 and C_4H_{10} are substantially higher over the study region. The September–February to March–August ratios are 3.2, 2.2, 1.9, 3.2, 2.3, and 2.4 for C_2H_6, C_2H_4, C_3H_8, C_3H_6, C_2H_2, and C_4H_{10}, respectively. However, in case of i-C_5H_{10}, CH_4 and CO, these ratios are 0.84, 1.1, and 1.3, respectively. Among the measured hydrocarbons, C_4H_{10} contributes about 29 % to the C_2–C_5 total, followed by C_3H_8 (25 %). Over Kolkata, the propylene equivalents, which are also an indicator of O_3 forming potential (Chameides et al. 1992), are highest for C_3H_6, followed by C_2H_4 and i-C_5H_{10}.

Source signatures from inter-species relationships

Table 4 presents the inter-species relationships among CO, SO_2, and hydrocarbons. To account for the impact of prevailing wind regimes, the data is divided into summer (March–August) and winter (September–February). Since it is likely that photochemistry can influence the relationships significantly (Leuchner and Rappenglück 2010), the table presents relationship based on all observations as well as observations excluding the noontime period (when photochemical activity is maximum). Excellent correlations are observed for butane isomers for both the seasons (Table 4). The slope matches the values (0.34–0.52) obtained over

several sites in UK which was attributed to evaporative emissions from petrol station refueling and refinery operations (Derwent et al. 2000). C_4H_{10} also shows good correlations with C_3H_8 (Table 4), alluding to LPG emissions (Table 1). Good correlation of n-C_4H_{10} with C_2H_2 confirms impact of vehicular emissions (Xie and Berkowitz 2006). Overall, strong correlations among C_3H_8, C_4H_{10}, and C_2H_2 suggest impacts of local vehicular emissions as well as influence of LPG. Associations between C_2H_4 and C_3H_8 suggest additional co-emissions from combustion sources. Strong correlations between CH_4, C_2H_6, and C_2H_4 during winter compared to pre-monsoon also indicate influence of combustion sources (biomass/biofuel).

CO is strongly correlated to CH_4, C_2H_6, C_2H_4, C_2H_2, and C_4H_{10} during winter indicating impacts of biomass/biofuel burning. Since not much biomass burning occurs during this period, it is more likely that biofuel burning along the east IGP is the major source of CO (Table 1). The C_2H_6/CO slope obtained in this study (0.007 ppbv/ppbv) is very close to the values obtained for Ahmedabad (0.008; Sahu and Lal 2006a) and Hissar (0.01; Lal et al. 2012) as well as Japan/Korea (Wang et al. 2004b). Further, C_2H_4 to CO slope of 0.02 obtained by Lal et al. (2012) is close to winter values obtained in this study indicating impacts of biofuel on CO values. However, there are bound to be significant impacts of fossil

Fig. 7 Daytime variations of CO, CH₄, and NMHCs (C₂–C₅) over Kolkata during March 2012– February 2013
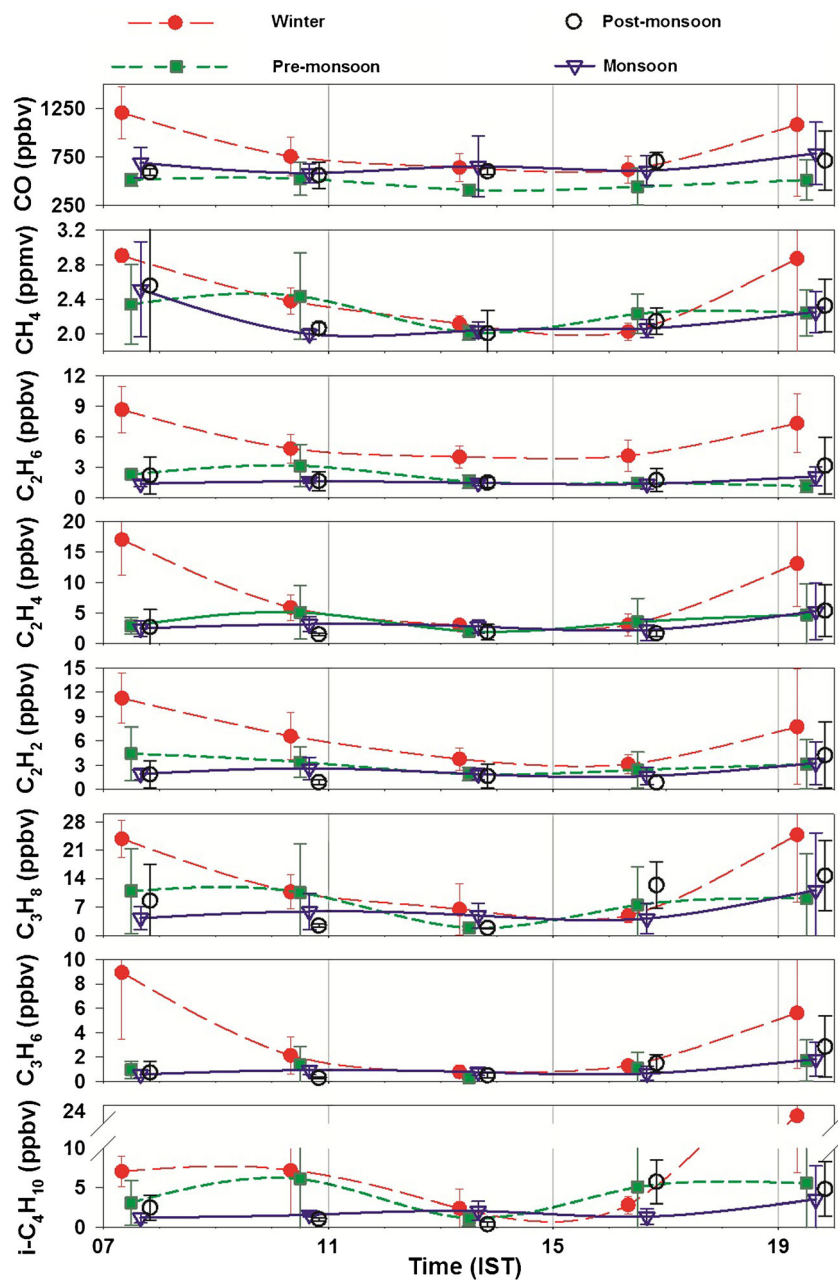
fuel combustions to CO levels in the IGP as suggested by low C_2H_6/C_3H_8 (slope=0.2, R^2=0.6) during winter. Good correlations also exist between CO, C_3H_8 and n-C_4H_{10} during winter, corroborating co-emissions from petrochemical industries/LPG sources (Table 1). Efficient mixing of various emissions from a plethora of collocated sources accompanied by boundary later dilution results in weak source signatures during pre-monsoon. Although the correlations of CO with hydrocarbons are very poor during pre-monsoon, the R^2 increases significantly when the data analysis excludes noontime values, indicating influence of photochemistry in CO–hydrocarbon relationships. Particularly

for CO-CH₄ relationship, when noontime data is excluded, the R^2 increases significantly for summer data but decreases for winter data. Nevertheless, source signatures can be difficult to interpret over urban regions, unless measurements of specific tracers like 3-methyl pentane (gasoline marker) or isoprene (biomass burning indicator) are available. The major difficulty in source interpretation over urban regions is that there could be a plethora collocated sources emitting the same gas.

The unique combination of SO₂, CO, and NMHC measurements allows to establish that SO₂ is more likely to be impacted by regional anthropogenic sources (power plants,

Table 4 Correlations between SO_2 (parts per billion by volume), CO (parts per billion by volume), CH_4 (parts per million by volume), and NMHCs (parts per billion by volume) over Kolkata for the period March 2012 to February 2013. The data is divided into two time periods (a) winter+postmonsoon, (b) premonsoon+monsoon. The analysis is given for two datasets, one including all data, the other excluding noontime data. The numbers in tables are presented in the format of slope (R^2)

Gas (X)	Gas (Y)	All data		Excluding noontime samples	
		Winter+postmonsoon	Premonsoon+monsoon	Winter+postmonsoon	Premonsoon+monsoon
No. of samples		23	48	18	41
n-C_4H_{10}	i-C_4H_{10}	0.40 (0.83)	0.59 (0.95)	0.39 (0.83)	0.60 (0.97)
C_3H_8	n-C_4H_{10}	0.66 (0.83)	0.51 (0.89)	0.63 (0.79)	0.52 (0.88)
C_2H_2	n-C_4H_{10}	1.37 (0.65)	1.81 (0.61)	1.35 (0.64)	0.95 (0.61)
C_3H_8	C_2H_2	0.31 (0.49)	0.22 (0.71)	0.33 (0.52)	0.21 (0.66)
C_3H_6	C_2H_4	0.07 (0.66)	0.06 (0.37)	0.06 (0.44)	0.05 (0.40)
C_3H_8	C_2H_4	0.42 (0.75)	0.33 (0.76)	0.41 (0.72)	0.35 (0.76)
CO	CH_4	1.4×10^{-3} (0.76)	4.0×10^{-4} (0.14)	1.1×10^{-3} (0.46)	5.6×10^{-4} (0.31)
CO	C_2H_6	6.7×10^{-3} (0.62)	1.6×10^{-3} (0.13)	7.0×10^{-3} (0.61)	2.2×10^{-3} (0.21)
CO	C_2H_2	0.016 (0.81)	3.3×10^{-3} (0.13)	0.015 (0.78)	4.4×10^{-3} (0.21)
CO	C_2H_4	0.02 (0.60)	5.7×10^{-3} (0.19)	0.02 (0.57)	6.8×10^{-3} (0.21)
CO	C_3H_8	0.02 (0.51)	0.02 (0.21)	0.02 (0.41)	0.02 (0.30)
CO	n-C_4H_{10}	0.02 (0.67)	9.9×10^{-3} (0.30)	0.01 (0.53)	0.01 (0.40)
CH_4	SO_2	10.37 (0.52)	1.44 (0.11)	7.52 (0.27)	1.92 (0.16)
C_2H_6	SO_2	1.88 (0.51)	0.67 (0.20)	2.25 (0.66)	1.03 (0.33)
C_3H_8	SO_2	0.36 (0.37)		0.39 (0.36)	
CO	SO_2	0.016 (0.53)		0.02 (0.68)	

industries, and refineries) rather than local emissions (transport, residential). This is because SO_2 is more strongly associated with CO and C_2H_6 and exhibits poorer correlations with gases emitted locally (C_3H_8, n-C_4H_{10} and C_2H_2) during winter. This is corroborated by PSCF analysis and weekday/weekend ratios. Nevertheless, being a major urban region, there would still be some local emissions of SO_2 impacting its background concentrations over Kolkata. The observed SO_2/CO slope during winter is lower than an estimate of 0.045 over China, which was attributed to coal burning (Wang et al. 2004b). This could be due to lower sulfur content of Indian coals.

Source apportionment from PMF analysis

Positive matrix factorization (PMF) is a multivariate factor analysis tool that decomposes a matrix of speciated sample data into matrices that facilitates grouping of sources based on observations at the receptor site (Paatero and Tapper 1994). In general, the PMF model provides robust results for the identification of sources in complex atmospheric environments (Leuchner and Rappengluck 2010). PMF v3.0 was utilized in this study using 10 species and 55 samples. In order to reduce the influence of photochemistry, the noontime

samples were excluded from the PMF analysis (Leuchner and Rappengluck 2010). Details regarding this method can be found in Ling et al. (2011) as well as Leuchner and Rappengluck (2010). The analysis resulted in six major factors (Fig. 8). Factor 1, dominated by CO and CH_4. Since CH_4 over Kolkata is not likely to be influenced much by agricultural sources, this factor connotes biofuel/biomass combustion (mainly biofuel). Factors 2 and 4, dominated by C_2H_2 and C_2H_4, seem to be related to traffic emissions (Ling et al. 2011). Factor 2 is dominated by alkenes and is related to petrochemistry while factor 4, dominated by C_2H_2 and C_2H_4, is more closely related to vehicle exhausts (Leuchner and Rappengluck 2010). Factor 3 is dominated by SO_2 and related to coal combustions (power plants and industries). However, abundance of C_2H_6 in factor 3 also indicates influence of natural gas and evaporation, which could occur from collocated emission sources followed by wind borne transport (it may be noted that significant correlations exist between SO_2 and C_2H_6, mainly during winter).

Factor 5 is dominated by i-C_5H_{10} and identified as fuel (mainly gasoline) evaporation (Table 1). Factor 6 is dominated by C_3H_8 and C_4H_{10} and this combination of species is typically found in liquefied petroleum gas (Table 1; Leuchner and Rappengluck 2010).

Fig. 8 Source profiles
(percentage of species total)
resolved with PMF analysis
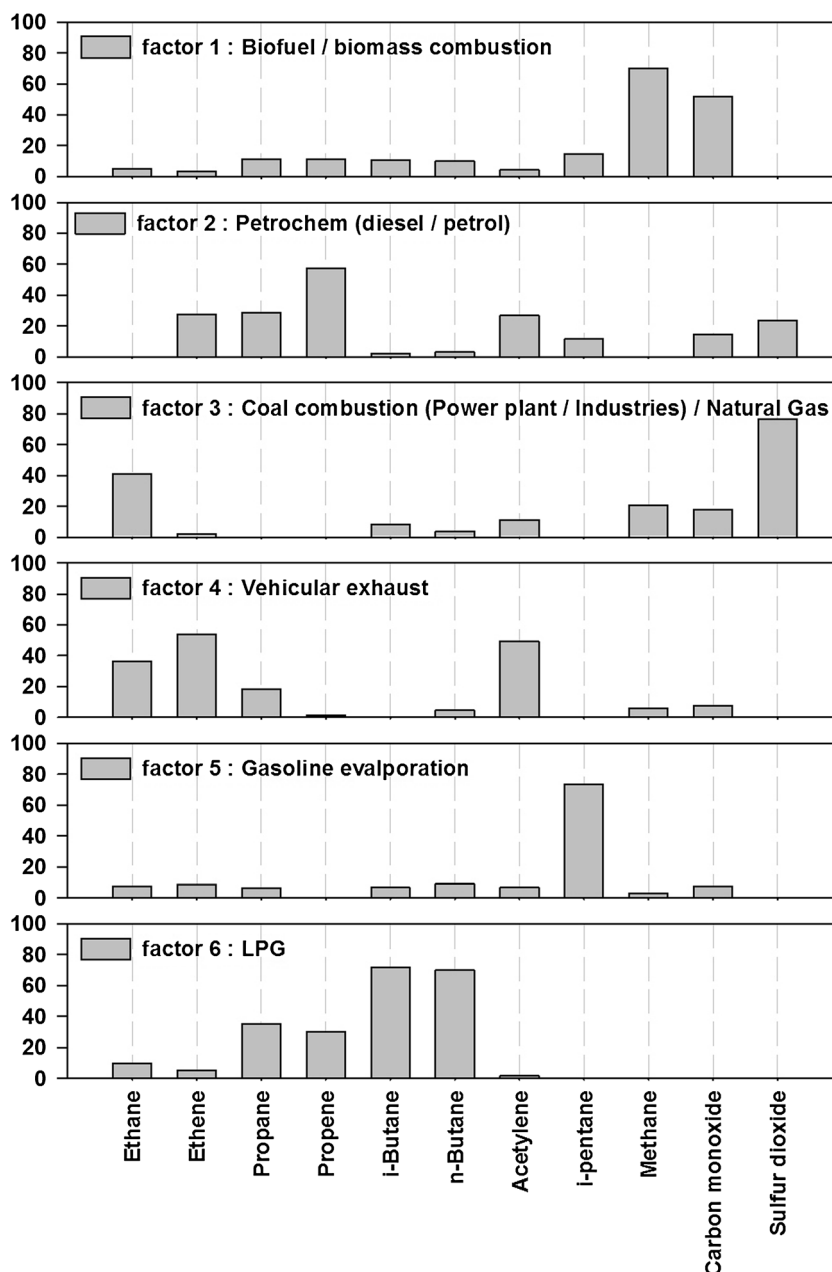
Conclusion

A year-long study of SO$_2$, CO, and hydrocarbons over Kolkata during 2012–2013 enabled interpretation of emission characteristics over this region. The observed SO$_2$ concentrations are comparable to several Asian sites but higher than European sites. High levels of SO$_2$ during winter (>6 ppbv) are attributed to regional emissions and subsequent trapping of these air masses favored by a stable atmosphere with low ventilation coefficient. Coal burning in industrial areas and power plants in eastern IGP are identified as potential source

regions for SO$_2$ during winter. Daytime elevations in SO$_2$ during summer seem to be related to photo-oxidation of RSCs from a nearby landfill region. The daytime enhancement in MOPITT derived CO over Kolkata during December (478 ppbv) over April (331 ppbv) is about 44 %, which is also reciprocated by in-situ, sample-based measurements during April (323 ppbv) and December (469 ppbv) for the year 2012. Early morning enhancements during winter for several trace gases indicate the role of MLD dynamics. Interspecies correlations show the dominant influence of LPG leakage and petrochemical industries to local air quality during winter

apart from vehicular traffic. Correlation analysis shows that CO is dominated by biofuel combustions. Overall, it may be concluded that the major emission sources of different gases are not collocated. The "sui generis" combination of measured species in this study has helped to segregate impacts of transport from local emissions. From the point of view of emission inventories, these measurements over Kolkata (the world's 16th largest megacity in terms of population) would be very useful for characterizing urban Indian emissions and potentially also represent South Asia. The concentrations over Kolkata may be interpreted as the end point of anthropogenic inputs to the IGP outflow into the BoB and subsequently the Indian Ocean during winter. Thus, these measurements (e.g., C_2H_2 to CO ratios) can serve as initial values to calculate photochemical processing of air masses over the BoB. Nevertheless, measurements of additional tracers, e.g., isoprene, methyl chloride, etc. are required to better characterize the emission scenarios over this region.

Highlights

- First time, simultaneous measurements of SO_2, CO, CH_4, and NMHCs over Kolkata, a megacity in SE Asia.
- Study discusses impacts of regional transport vs local emissions of pollutants
- SO_2 diurnal variations influenced by photo-oxidation and boundary layer dynamics.
- SO_2 concentrations impacted by regional emissions from coal combustions.
- Inter-species correlations are used for source apportionment.

References

Adhikary B et al. (2007) Characterization of the seasonal cycle of south Asian aerosols: a regional-scale modeling analysis. J Geophys Res 112: D22S22. doi:10.1029/2006JD008143.

Apel EC et al (2010) Chemical evolution of volatile organic compounds in the outflow of the Mexico City Metropolitan area. Atmos Chem Phys 10:2353–2376

Barletta B et al (2002) Mixing ratios of volatile organic compounds (VOCs) in the atmosphere of Karachi, Pakistan. Atmos Environ 36:3429–3443

Blake DR, Rowland FS (1995) Urban leakage of liquefied petroleum gas and its impact on Mexico City air quality. Science 269:953–956

Chameides WL et al (1992) Ozone precursor relationships in the ambient air. J Geophys Res 97:6037–6055

Chin M, Jacob DJ (1996) Anthropogenic and natural contributions to tropospheric sulfate. J Geophys Res 101(D13):18691–18699

Datta A et al (2011) Variation of ambient SO_2 over Delhi. J Atmos Chem. doi:10.1007/s10874-011-9185-2

De Bruyn WJ et al (2006) DMS and SO_2 measurements in the tropical marine boundary layer. J Atmos Chem 53:145–154

Derwent RG et al (2000) Analysis and interpretation of the continuous hourly monitoring data for 26 C2–C8 hydrocarbons at 12 United Kingdom sites during 1996. Atmos Environ 34:297–312

Duncan BN et al (2007) Global budget of CO, 1988–1997: source estimates and validation with a global model. J Geophys Res 112, D22301. doi:10.1029/2007JD008459

Faloona I (2009) Sulfur processing in the marine atmospheric boundary layer: a review and critical assessment of modeling uncertainties. Atmos Environ 43:2841–2854

Forster P et al (2007) Changes in atmospheric constituents and in radiative forcing. IPCC, In

Garg A et al (2001) Subregion (district) and sector level SO_2 and NO_x emissions for India: assessment of inventories and mitigation flexibility. Atmos Environ 35:703–713

Guo H et al (2007) C1–C8 volatile organic compounds in the atmosphere of Hong Kong: overview of atmospheric processing and source apportionment. Atmos Environ 41:1456–1472

Gupta AK, Patil RS, Gupta SK (2003) A long-term study of oxides of nitrogen, sulphur dioxide, and ammonia for a port and harbor region in India. J Environ Sc Healt Part A 38(12):2877–2894

Gurjar BR, Butler TM, Lawrence MG, Lelieveld J (2008) Evaluation of emissions and air quality in megacities. Atmos Environ 42(7):1593–1606

Guttikunda SK et al (2001) Sulfur deposition in Asia: seasonal behavior and contributions from various energy sectors. Water Air Soil Pollut 131:336–406

Hanke M et al (2003) Atmospheric measurements of gas-phase HNO_3 and SO_2 using chemical ionization mass spectrometry during the MINATROC field campaign 2000 on Monte Cimone. Atmos Chem Phys 3:417–436

Horowitz LW et al (2003) A global simulation of tropospheric ozone and related tracers: description and evaluation of MOZART, version 2. J Geophys Res 108:4784. doi:10.1029/2002JD002853

Lal S et al (2012) Light non-methane hydrocarbons at two sites in the Indo-Gangetic Plain. J Environ Monit 14:1159

Leuchner M, Rappenglück B (2010) VOC Source-receptor relationships in Houston during TexAQS-II. Atmos Environ 44: 4056–4067.

Ling ZH et al (2011) Sources of ambient volatile organic compounds and their contributions to photochemical ozone formation at a site in the Pearl River Delta, southern China. Environ Poll 159:2310–2319

Lu Z, Zhang Q, Streets DG (2011) Sulfur dioxide and primary carbonaceous aerosol emissions in China and India, 1996–2010. Atmos Chem Phys 11:9839–9864, doi:10.5194/acp-11-9839-2011, 2011

Matsuda K et al (2006) Deposition velocity of O_3 and SO_2 in the dry and wet season above a tropical forest in northern Thailand. Atmos Environ 40:7557–7564

Mallik C, Venkataramani S, Lal S (2012) Study of a high SO_2 event observed over an urban site in western India. Asia-Pac J Atmos Sci 48(2):171–180. doi:10.1007/s13143-012-0017-3

Mallik C, Lal S (2013) Seasonal characteristics of SO_2, NO_2 and CO emissions in and around the Indo-Gangetic Plain. Env Monit Assess 186(2):1295–1310

Mallik C, Lal S, Venkataramani S, Naja M, Ojha N (2013) Variability in ozone and its precursors over the Bay of Bengal during post-monsoon: transport and emission effects. J of Geophy Res 118(17):10190–10209

Meng ZY et al (2010) Ambient sulfur dioxide, nitrogen dioxide, and ammonia at ten background and rural sites in China during 2007–2008. Atmos Environ 44(21–22):2625–2631

Mohn J, Emmenegger L (2001) Determination of sulfur doixide by pulsed UV-Fluorescence. Swiss Federal Laboritories for Materials Testing & Research.

Naja M, Lal S, Chand D (2003) Diurnal and seasonal variabilities in surface ozone at a high altitude site Mt Abu (24.6° N, 72.7° E, 1680 m asl) in India. Atmos Environ 37:4205–4215

Nguyen HT, Kim KH (2006) Evaluation of SO$_2$ pollution levels between four different types of air quality monitoring stations. Atmos Environ 40:7066–7081

Paatero P, Tapper U (1994) Positive matrix factorization: a non-negative factor model with optimal utilization of error estimates of data values. Environmetrics 5:111–126

Rai A, Ghosh S, Chakraborty S (2010) Wet scavenging of SO$_2$ emissions around India's largest lignite based power plant. Adv Geosci 25:65–70

Rao A et al (1997) Non-methane hydrocarbons in industrial locations of Bombay. Atmos Environ 31:1077–1085

Rudolph J (1995) The tropospheric distribution and budget of ethane. J Geophys Res 100(D6):11369–11381

Sahu LK, Lal S (2006a) Distributions of C2–C5 NMHCs and related trace gases at a tropical urban site in India. Atmos Environ 40:880–891

Sahu LK, Lal S (2006b) Characterization of C2–C4 NMHCs distributions at a high altitude tropical site in India. J Atmos Chem 54:161–175

Saliba NA et al (2006) Variation of selected air quality indicators over the city of Beirut, Lebanon: assessment of emission sources. Atmos Environ 40:3263–3268

Sawada S, Totsuka T (1986) Natural and anthropogenic sources and fate of atmospheric ethylene. Atmos Environ 20:821–832

Schneidemesser E, Monks PS, Plass-Duelmer C (2010) Global comparison of VOC and CO observations in urban areas. Atmos Environ 44:5053–5064

Streets DG et al (2003) An inventory of gaseous and primary aerosol emissions in Asia in the year 2000. J Geophys Res 108(D21):8809. doi:10.1029/2002jd003093

Swamy YV et al (2012) Impact of nitrogen oxides, volatile organic compounds and black carbon on atmospheric ozone levels at a semi arid urban site in Hyderabad. Aerosol Air Qual Res 12:662–671

Wang TJ et al (2003) Atmospheric sulfur deposition and the sulfur nutrition of crops at an agricultural site in Jiangxi province of China. Tellus 55B:893–900

Wang JS et al (2004a) A 3-D model analysis of the slowdown and interannual variability in the methane growth rate from 1988 to 1997. Glob Biogeochem Cyc 18, GB3011. doi:10.1029/2003GB002180

Wang T et al. (2004b) Relationships of trace gases and aerosols and the emission characteristics at Lin'an, a rural site in eastern China, during spring 2001. J Geophys Res 109: D19S05. doi:10.1029/2003JD004119.

Wang YQ, Zhang XY, Draxler R (2009) TrajStat: GIS-based software that uses various trajectory statistical analysis methods to identify potential sources from long-term air pollution measurement data. Environ Modell Soft 24:938–939

Xiao Y, Jacob DJ, Turquety S (2007) Atmospheric acetylene and its relationship with CO as an indicator of air mass age. J Geophys Res 112, D12305. doi:10.1029/2006JD008268

Xie YL, Berkowitz CM (2006) The use of positive matrix factorization with conditional probability functions in air quality studies: an application to hydrocarbon emissions in Houston, Texas. Atmos Environ 40(17):3070–3091. doi:10.1016/j.atmosenv.2005.12.065

Xue L et al (2011) Vertical distributions of non-methane hydrocarbons and halocarbons in the lower troposphere over northeast China. Atmos Environ 45:6501–6509